Journal of
Synchrotron Radiation

ISSN 0909-0495

Received 9 January 2009
Accepted 17 March 2009

Origin of the X-ray magnetic circular dichroism at the *L*-edges of the rare-earths in $R_xR'_{1-x}Al_2$ systems

Jesús Chaboy,[a,b]* María Ángeles Laguna-Marco,[c] Cristina Piquer,[a,d] Roberto Boada,[a,b] Neculai Plugaru,[d,e] Hiroshi Maruyama[f] and Naomi Kawamura[g]

[a]Instituto de Ciencia de Materiales de Aragón, CSIC-Universidad de Zaragoza, 50009 Zaragoza, Spain, [b]Departamento de Fisica de la Materia Condensada, Universidad de Zaragoza, 50009 Zaragoza, Spain, [c]Advanced Photon Source, Argonne National Laboratory, Argonne, IL 60439, USA, [d]Departamento de Ciencia y Tecnología de Materiales y Fluidos, Universidad de Zaragoza, 50009 Zaragoza, Spain, [e]National Institute of Materials Physics, PO Box MG-07, Bucharest, Romania, [f]Graduate School of Science, Hiroshima University, 1-3-1 Kagamiyama, Higashi-Hiroshima 739-8526, Japan, and [g]Japan Synchrotron Radiation Research Institute/SPring-8, 1-1-1 Kouto, Sayo, Hyogo 679-5198, Japan. E-mail: jchaboy@unizar.es

An X-ray magnetic circular dichroism (XMCD) study performed at the rare-earth $L_{2,3}$-edges in the $R_xR'_{1-x}Al_2$ compounds is presented. It is shown that both R and R' atoms contribute to the XMCD recorded at the L-edges of the selected rare-earth, either R or R'. The amplitude of the XMCD signal is not directly correlated to the magnetization or to the value of the individual (R, R') magnetic moments, but it is related to the molecular field acting on the rare-earth tuned in the photoabsorption process. This result closes a longstanding study of the origin of the XMCD at the L-edge of the rare-earths in multi-component systems, allowing a full understanding of the exact nature of these signals.

Keywords: X-ray magnetic circular dichroism; rare-earth *L*-edges.

1. Introduction

In recent years the advent of new synchrotron radiation sources has led to the development of magnetic studies on the microscopic scale by using X-ray core-level spectroscopies such as X-ray circular magnetic dichroism (XMCD) (Lovesey & Collins, 1996; Stöhr, 1999; Kortright *et al.*, 1999; Funk *et al.*, 2005). The great advantage of using X-rays lies in the fact that each element can be probed separately since the energy of the X-ray absorption edges is characteristic for each element. XMCD combined with the so-called sum rules may provide element-specific information about the orbital (Thole *et al.*, 1992) and spin (Carra *et al.*, 1993) magnetic moments of the states of the absorbing atom probed in the absorption process.

In this way, XMCD has been mostly applied to those cases in which the final states are localized, such as the *d*-states ($L_{2,3}$-edges) of the late transition metals like Co and Ni (Lovesey & Collins, 1996; Stöhr, 1999; Kortright *et al.*, 1999; Chen *et al.*, 1993). However, the application of the spin sum rule (Carra *et al.*, 1993) worsens in other cases because of two main problems: the unknown value of the magnetic dipole operator T_z and the need for a large $L_{2,3}$-edge spin–orbit splitting. This $2p$ spin–orbit splitting is strongly reduced for light transition metals, and quantum mechanical mixing of $j_{3/2}$ and $j_{1/2}$ excitations is present. This mixing reduces the observed XMCD related spin and magnetic dipole term contributions and prevents the direct application of XMCD spin sum rules (Goering, 2005; Crocombettey *et al.*, 1996). Moreover, the strong electron core-hole correlations in the early $3d$ transition metals lead to dramatic changes in the spectral intensities and a severe deviation of the spin sum rule (Scherz *et al.*, 2004).

The problem of extracting quantitative magnetic information from the XMCD spectra increases in those cases in which the final states are delocalized, such as the $4p$ states (K-edge) of the $3d$ transition metals (T) and the $5d$ states ($L_{2,3}$-edges) of the rare-earths (R). Initially, the Fe K-edge XMCD was thought to be proportional to the p-projected spin density of states (Schütz *et al.*, 1987). However, this interpretation failed to account for the cases of Co and Ni (Schütz & Wienke, 1989; Schütz *et al.*, 1989; Stähler *et al.*, 1993). According to Igarashi & Hirai, who pointed out the critical role of the hybridization of the $4p$ states with the $3d$ states at neighbouring sites (Igarashi & Hirai, 1994, 1996), the shape of the XMCD spectrum near the K-edge of the ferromagnetic metals such as Fe, Co and Ni is determined by the $3d$-projected orbital magnetization density of states. On the other hand, two main problems limit the use of XMCD for studying the magnetic properties of the $5d$ states of the rare-earths by using XMCD at the R $L_{2,3}$-edges. Both the contribution of quadrupolar transitions (Carra *et al.*, 1991; Lang *et al.*, 1992, 1994, 1995; Chaboy *et al.*, 1998*a*) and the spin dependence of the radial matrix elements of the dipolar transitions (Wang *et al.*, 1993) affect both the shape and the sign of the XMCD signals. The

appearance of these effects prevents the determination of the 5*d* magnetic moments from the simple application of the sum rules and, moreover, the correct determination of the sign of the magnetic coupling (Schütz *et al.*, 1988).

These problems become more acute when both localized and delocalized moments are present in the material, as in the case of *R*–*T* intermetallics (Laguna-Marco, 2007). Several works have shown that the rare-earth contributes to the XMCD spectrum recorded at the *T K*-edge (Chaboy *et al.*, 1996, 1998*b*, 2003, 2004, 2007*a*,*d*; Laguna-Marco *et al.*, 2005*a*, 2007; Ishimatsu *et al.*, 2007; Rueff *et al.*, 1998) and, conversely, the transition metal contributes to the XMCD signals recorded at the rare-earth $L_{2,3}$-edges (Laguna-Marco *et al.*, 2005*b*, 2008*a*,*b*; Giorgetti *et al.*, 2004; Chaboy *et al.*, 2008; Boada *et al.*, 2009*a*). The systematic work performed to date has demonstrated the universality of this behaviour within the *R*–*T* intermetallics. However, while the shape of these contributions does not depend significantly on the particular *R*/*T* stoichiometry, especially at the *R L*-edges, their amplitude shows a strong variation through different series. Indeed, in several cases of pure RT_2 compounds (*T* = Fe, Co) the rare-earth contribution to the *T K*-edge XMCD spectra is so large as to hinder that of the *T* 4*p* states that, however, are still present as demonstrated in the $(R_xLu_{1-x})Fe_2$ series by diluting the magnetic rare-earth with a non-magnetic one (Boada *et al.*, 2009*b*). This contribution is associated with the exchange interaction with the rare-earth, being mainly determined by the magnitude of the molecular field that the rare-earth magnetic moments cause at the *T* sites (Laguna-Marco *et al.*, 2009). A similar scheme was applied to the case of the *T* contribution to the rare-earth $L_{2,3}$-edges XMCD. Our results have shown that it is possible to establish a relationship between the *T* contribution to the rare-earth $L_{2,3}$-edges XMCD and the molecular field acting on the absorbing sites (Chaboy *et al.*, 2007*b*). These results suggest the possibility of extracting quantitative magnetic information from the analysis of the rare-earth $L_{2,3}$-edges XMCD, especially regarding both the exchange interaction between the 5*d* moments and those of the matrix, and also on the *R*(5*d*)–*T*(*d*) hybridization.

The experiments above have been performed in systems in which there is competition between the localized 4*f* magnetism of the rare-earth and the itinerant magnetism of the transition metal, and in which the *R*(5*d*)–*T*(*d*) hybridization plays a fundamental role into governing the magnetic properties of the compounds (Campbell, 1972; Yamada *et al.*, 1984; Yamada & Shimizu, 1985). However, similar behaviour has been observed in the $R(Al_{1-x}T_x)_2$ Laves phases (Laguna-Marco, 2007; Laguna-Marco *et al.*, 2007*a*,*b*, 2009) in which the magnetism shows an evolution from RKKY-like to itinerant magnetism. Therefore, we have tailored the study of the relationship between the XMCD signals recorded at the $L_{2,3}$-edges of the rare-earths and the magnetic properties of systems in which no *T*-3*d* magnetic moment and, consequently, no *R*(5*d*)–Fe(3*d*) hybridization are present. In this way, the systematic XMCD study performed on the RAl_2 series has shown that there is a clear relationship between the rare-earth L_2-edge XMCD and the molecular field coefficients n_{RR} (Laguna-Marco *et al.*, 2008*b*). More specifically, our results showed that the intensity of the *R* L_2 XMCD spectra remarkably mimics the modification of the n_{RR} coefficient through the RAl_2 series, which suggests that analysis of the XMCD signal can be used to obtain valuable information about the *R*(4*f*)–*R*(5*d*) exchange.

In order to go further in this subject we have extended our previous studies to the case of the substituted $R_{1-x}R'_xAl_2$ compounds. Here we present an XMCD study performed at the rare-earth $L_{2,3}$-edges in the $R_xR'_{1-x}Al_2$ compounds. The magnetic behaviour of these systems is accounted for in terms of the RKKY interaction and, consequently, it is not expected that the hybridization of the 5*d* states plays a significant role. However, our results show that in the case of the substituted $Gd_{1-x}R'_xAl_2$ compounds (with *R*′ = Dy, Ho, Er) the amplitude of the Gd $L_{2,3}$-edge XMCD spectra decreases upon doping despite the magnetization of the system increasing. In contrast, the substitution of Gd by *R*′ entails a strong modification of the magnetic ordering temperature, which indicates that the exchange interaction is strongly modified with respect to that of the undoped RAl_2 compounds. In this work it is shown that the observed decrease in the amplitude of the Gd $L_{2,3}$-edge XMCD is due to an *R*′ contribution, whose intensity is correlated with the molecular field that the *R*′ atoms exert on the Gd sublattice. Hence, our experimental findings provide a deeper insight into the interpretation of the $L_{2,3}$-edge XMCD spectra of the rare-earths by showing that the amplitude of the XMCD signals can be quantitatively related to the magnetic properties of the systems under study. In this way we have proven that these signals are determined not only by the magnetization of the probed sublattice but also by the other magnetic moments present in the material which should be considered in terms of the molecular field acting on the absorbing sites. These results open the possibility of using XMCD at the rare-earth $L_{2,3}$-edges to extract experimentally quantitative magnetic information.

2. Experimental

RAl_2 compounds (*R* = Pr, Nd, Sm, Gd, Tb, Dy, Ho and Er) were prepared by melting the pure elements in a high-frequency induction furnace, under Ar protective atmosphere. The as-cast alloys were wrapped in Ta foil and enclosed in silica tubes, under Ar gas. All the alloys were annealed at 1073 K for 100 h and then quenched to room temperature. A similar procedure was applied to the synthesis of the $Gd_{1-x}R_xAl_2$ compounds (*R* = Dy, Ho, Er and Lu) that were annealed at 1023 K for one week. Structural characterization was performed at room temperature by means of powder X-ray diffraction, using a rotating-anode Rigaku diffractometer in the Bragg–Brentano geometry, with Cu $K\alpha$ radiation. The magnetic measurements were performed by using a commercial SQUID magnetometer (Quantum Design MPMS-5s). Magnetic isotherms were measured on loose powders in applied magnetic fields $H \leq 5$ T.

XMCD experiments were performed at the beamline BL39XU of the SPring-8 facility (Maruyama, 2001). For the

measurements, homogeneous layers of the powdered samples were made by spreading fine powders of the material onto adhesive tape. The thickness and homogeneity of the samples were optimized to obtain the best signal-to-noise ratio, giving a total absorption jump of $\sim$1 at about 150 eV above the edge. In all of the cases, the origin of the energy scale, E_0, was chosen at the inflection point of the absorption edge, and the XAS spectra were normalized to the averaged absorption coefficient at high energy. The XMCD spectra were recorded at different fixed temperatures in the transmission mode using the helicity-modulation technique (Suzuki *et al.*, 1998). The sample was magnetized by an external magnetic field, $H = 2$ T, applied in the direction of the incident beam, and the helicity was changed from positive to negative at each energy point. In this way the spin-dependent absorption coefficient was obtained as the difference of the absorption coefficient, $\mu_c = (\mu^- - \mu^+)$, for antiparallel, μ^-, and parallel, μ^+, orientation of the photon helicity and sample magnetization. For the sake of accuracy, the direction of the applied magnetic field was reversed to obtain the XMCD, now corresponding to $\mu_c = (\mu^+ - \mu^-)$, by switching the helicity. Subtraction of the XMCD spectra recorded for both field orientations cancels, if present, any spurious signal.

3. Results and discussion

Both $R\mathrm{Al}_2$ and $R_{1-x}R'_x\mathrm{Al}_2$ series of compounds crystallize in the cubic Laves C15 $MgCu_2$ structure. The diffraction patterns were Rietveld refined using the *FULLPROF* code (Rodriguez-Carvajal, 1993). All the samples were found to be single phase and the cell parameters were determined from the X-ray diffraction patterns (see Fig. 1). The cell parameters of both the $R\mathrm{Al}_2$ and the $\mathrm{Gd}_{1-x}R_x\mathrm{Al}_2$ compounds are summarized in Table 1. As shown in Fig. 1, the cell volume of the pure $R\mathrm{Al}_2$ compounds decreases as the atomic number increases, as expected because of the lanthanide contraction. In addition, the cell parameters of the $\mathrm{Gd}_{1-x}R_x\mathrm{Al}_2$ compounds follow a linear variation with the composition (x) between the end-members, in agreement with Vegard's law.

The temperature dependence of the magnetization through the $R\mathrm{Al}_2$ series is shown in Fig. 2 together with the magnetization *versus* applied magnetic field curves recorded at 4.2 K. The $R\mathrm{Al}_2$ compounds order ferromagnetically. The magnetic order temperature, T_C, of the series scales well with the de Gennes factor $(g-1)^2J(J+1)$ (de Gennes, 1966), in agreement with the predictions of the simple RKKY model. This result indicates that the magnetic order is mainly driven by the R sublattice, which differs from the isomorphous $R\mathrm{Fe}_2$ compounds where magnetic order is governed by the itinerant subsystem. The magnetic moments of these compounds are slightly smaller than the corresponding free rare-earth ion values, gJ, indicating some crystal field quenching (Purwins & Leson, 1990). The results summarized in Fig. 2 and Table 1 are in agreement with the numerous investigations that have been performed on $R\mathrm{Al}_2$ compounds (Buschow, 1979; Purwins & Leson, 1990).

Table 1
Main structural and magnetic parameters of the $R\mathrm{Al}_2$ and $R_{1-x}R'_x\mathrm{Al}_2$ compounds: lattice constant (a), unit-cell volume (V), Curie temperature (T_C) and the magnetization measured at $T = 4.2$ K and $H = 5$ T (M_{5T}).

Compound	a (Å)	V (Å^3)	T_C (K)	M_{5T} (μ_B/f.u.)
$PrAl_2$	8.028	517.3	33	2.94
$NdAl_2$	8.001	512.1	79	2.39
$SmAl_2$	7.942	501.0	64	0.24
$GdAl_2$	7.898	492.6	164	6.74
$TbAl_2$	7.863	486.1	109	8.90
$DyAl_2$	7.837	481.4	58	9.64
$HoAl_2$	7.812	476.8	29	9.20
$ErAl_2$	7.791	472.9	13	7.63
$Gd_{0.75}Dy_{0.25}Al_2$	7.880	489.3	145	8.37
$Gd_{0.50}Dy_{0.50}Al_2$	7.864	486.2	115	8.76
$Gd_{0.75}Ho_{0.25}Al_2$	7.874	488.2	141	8.46
$Gd_{0.50}Ho_{0.50}Al_2$	7.855	484.7	101	8.64
$Gd_{0.75}Er_{0.25}Al_2$	7.875	488.4	135	7.80
$Gd_{0.50}Er_{0.50}Al_2$	7.839	481.7	94	7.73
$Gd_{0.75}Lu_{0.25}Al_2$	7.856	484.8	128	5.26

Within the series, $GdAl_2$ exhibits the highest Curie temperature ($T_C = 164$ K). This fact, and the absence of any significant effect of crystal fields on the S state of the Gd^{3+} ion (Burd & Lee, 1977), makes $GdAl_2$ a good candidate for studying systematically the effect of replacing Gd by a different rare-earth. Hence, we have synthesized the $\mathrm{Gd}_{1-x}R_x\mathrm{Al}_2$ compounds in which Gd is replaced by Dy, Ho, Er and non-magnetic Lu. The dilution of Gd by Lu is expected to act as a simple magnetic dilution effect because Lu carries no

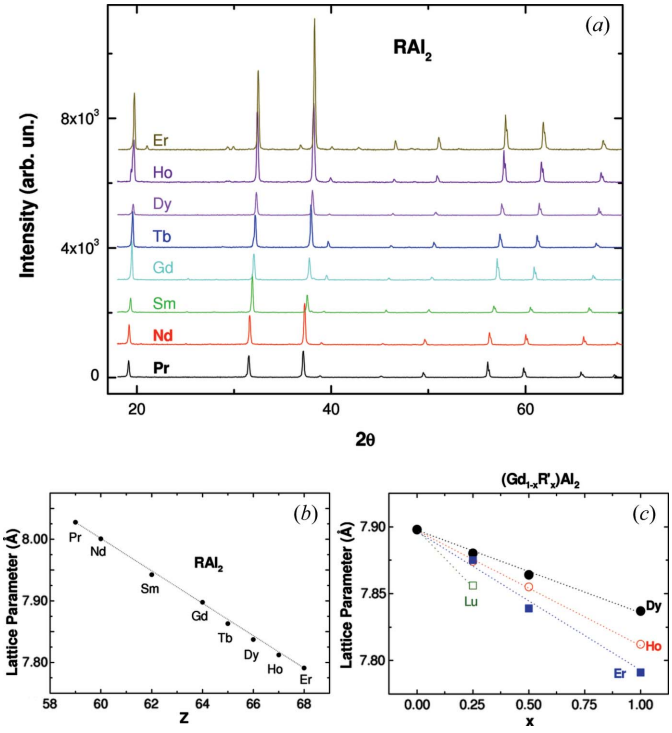

Figure 1
(*a*) X-ray powder diffraction patterns of the $R\mathrm{Al}_2$ series. (*b*) Variation of the lattice parameter through the $R\mathrm{Al}_2$ series. (*c*) Dependence of the lattice parameter on the rare-earth substitution in the $\mathrm{Gd}_{1-x}R'_x\mathrm{Al}_2$ [R' = Dy (filled circles), Ho (red, open circles), Er (blue, filled squares) and Lu (green, open squares)] series. This figure is in colour in the electronic version of this paper.

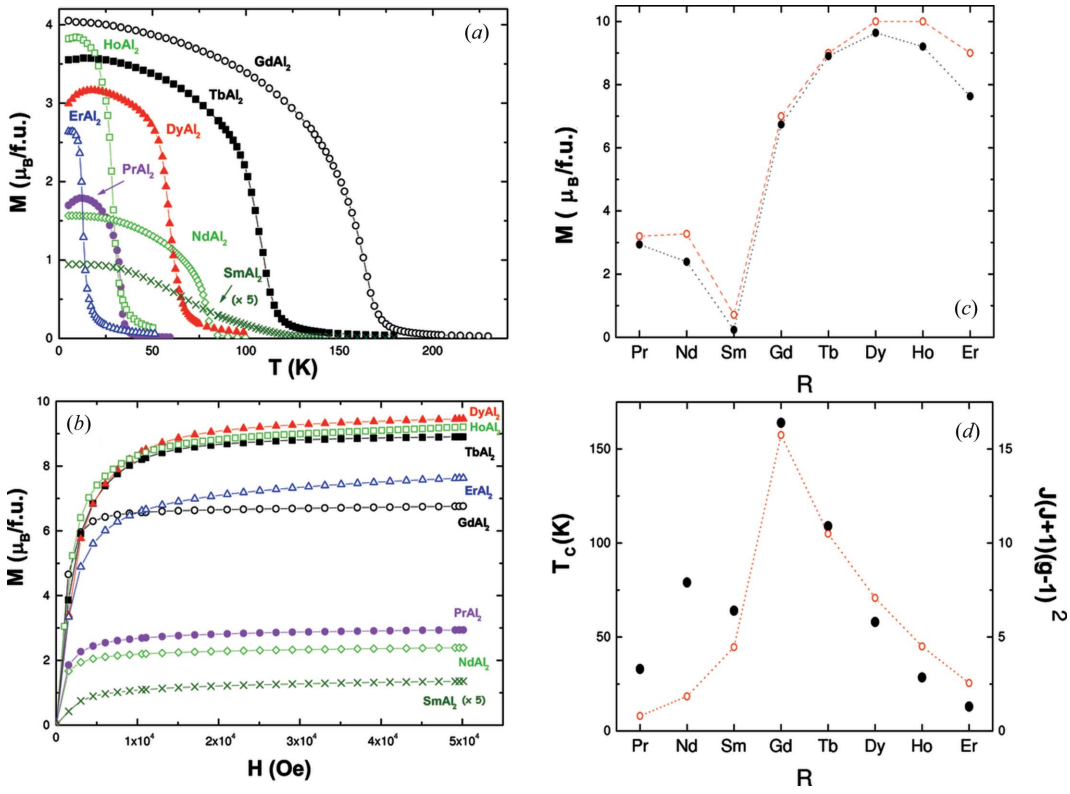

Figure 2
(*a*) Temperature dependence of the magnetization of the $R\mathrm{Al}_2$ compounds measured under an applied magnetic field $H = 0.1$ T. (*b*) Magnetization *versus* applied magnetic field curves of the $R\mathrm{Al}_2$ compounds recorded at $T = 4.2$ K. (*c*) Comparison of the magnetization of the $R\mathrm{Al}_2$ at $T = 4.2$ K and $H = 5$ T (black, filled circles) and the free-ion μ_{4f} magnetic moments (red, open circles). (*d*) Comparison of the Curie temperatures of the $R\mathrm{Al}_2$ compounds (red, open circles) and the $J(J+1)(g-1)^2$ dependence (black, filled circles) through the series. This figure is in colour in the electronic version of this paper.

magnetic moment and the magnetic state of Gd is thought to remain unaffected by the substitution. For a 25% Lu substitution, the magnetization decreases from 6.74 μ_B/f.u. in GdAl_2 to 5.26 μ_B/f.u. Hence, it is 78% of the magnetization of the parent compound, in agreement with the expected magnetic dilution effect. A similar reduction is found for the magnetic order temperature that decreases from 164 K in GdAl_2 to 128 K in $\mathrm{Gd}_{0.75}\mathrm{Lu}_{0.25}\mathrm{Al}_2$ (see Fig. 3).

In the case of the substitution of Gd by a magnetic rare-earth, the ferromagnetic order is preserved although the substitution has different consequences regarding both the magnetization and the magnetic ordering temperature of the systems. The magnetization of $\mathrm{Gd}_{1-x}R_x\mathrm{Al}_2$ is reinforced with respect to what is expected from the addition of the magnetization of both $R\mathrm{Al}_2$ and $R'\mathrm{Al}_2$ pure compounds according to a two-sublattice model. Within this framework, it is assumed

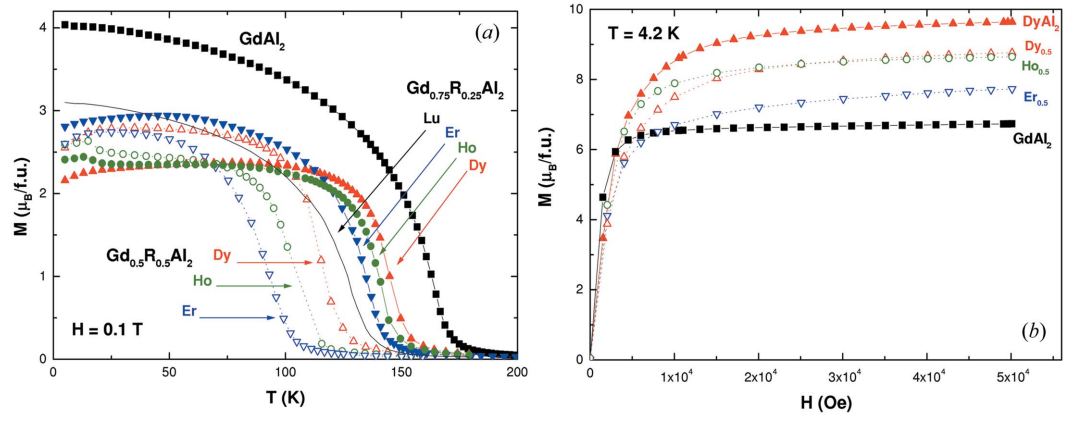

Figure 3
(*a*) Temperature dependence of the magnetization of the $\mathrm{Gd}_{1-x}R'_x\mathrm{Al}_2$ compounds measured under an applied magnetic field $H = 0.1$ T: R' = Er (blue, filled down triangles), Ho (green, filled circles) and Dy (red, filled triangles); and $x = 0.25$ (solid symbols); $x = 0.5$ (open symbols). (*b*) Comparison of the magnetization *versus* applied magnetic field curves of the pure $R\mathrm{Al}_2$ (solid symbols) and $\mathrm{Gd}_{0.5}R'_{0.5}\mathrm{Al}_2$ (open symbols) compounds for R' = Er (blue, open down triangles), Ho (green, open circles) and Dy (red, open triangles). This figure is in colour in the electronic version of this paper.

that the total magnetization of the $Gd_{0.5}R'_{0.5}Al_2$ compounds corresponds to the weighted addition of the magnetization of the parent single compounds, $M_{Tot} = 0.5M(GdAl_2) + 0.5M(R'Al_2)$. In the case of $Gd_{0.5}Dy_{0.5}Al_2$, this model yields $M_{Calc} = 8.19\ \mu_B$/f.u., while the measured magnetization at $T = 4.2$ K and $H = 5$ T is $M_{exp} = 8.76\ \mu_B$/f.u. The same trend is found for both $Gd_{0.5}Ho_{0.5}Al_2$, $M_{exp} = 8.64$ *versus* M_{Calc} $7.97\ \mu_B$/f.u., and $Gd_{0.5}Er_{0.5}Al_2$, $M_{exp} = 7.73$ *versus* M_{Calc} $7.19\ \mu_B$/f.u. Interestingly, a better agreement is found if the magnetization is calculated by using the 4*f* free-ion magnetic moments values: $M_{Calc} = 8.5\ \mu_B$/f.u. for Dy and Ho, and $8\ \mu_B$/f.u. for Er. These results indicate that the rare-earth ions in the $Gd_{0.5}R'_{0.5}Al_2$ compounds retain their magnetic properties upon dilution. However, the modification of the magnetic ordering temperature indicates that the exchange interaction is strongly modified with respect to that of the RAl_2 compounds.

This situation represents the best starting point to study the relationship between the rare-earth $L_{2,3}$-edge XMCD signals and the magnetic properties of the materials. In principle, if the amplitude of the XMCD signal was proportional to the magnetic moment of the absorbing atom or to the magnetization of the compound, no significant variation of the amplitude of the XMCD signal recorded at the Gd $L_{2,3}$-edges through the $Gd_{0.5}R'_{0.5}Al_2$ series would be expected. The total magnetization of the systems increases after the Gd substitution. Therefore, the amplitude of the XMCD signals should be increased through the $Gd_{0.5}R'_{0.5}Al_2$ series. By contrast, if the amplitude of the XMCD signals was determined by the exchange interaction, a strong modification of the XMCD amplitude should be expected. In this respect, we show in Fig. 4 the XMCD spectra recorded at the Gd L_2-edge in the investigated $Gd_{0.5}R'_{0.5}Al_2$ compounds. The Gd L_2-edge XMCD spectrum shows in all cases a main negative peak at the edge. This spectral profile is similar for all the compounds and only the amplitude of the signal is modified upon substitution of Gd by another lanthanide. Similar results are found at the Gd L_3-edge. In this case, the XMCD is positive and its intensity is one half of the L_2 one. Moreover, the intensity of the main peak of the XMCD spectrum and the integral of the signal over all the experimental range scale perfectly at both the L_2- and L_3-edges. Therefore, the modification of the amplitude of the XMCD spectra will be referred hereafter to the intensity values.

As shown in Fig. 4, the intensity of the Gd L_2-edge XMCD in $Gd_{0.75}Lu_{0.25}Al_2$ is ~90% of that in $GdAl_2$. However, the intensity of the XMCD signal markedly decreases through the $Gd_{0.5}R'_{0.5}Al_2$ series. Compared with that of $GdAl_2$, its amplitude is ~80%, 50% and 25% for Dy, Ho and Er, respectively. Such a variation is not expected in terms of the diminution of the Gd magnetic moment. Similarly, this behaviour is not expected on the basis of the modification of the total magnetization, which increases after substitution. It might be argued that the magnetization at the working temperatures departs from the relation found at $T = 4.2$ K and $H = 5$ T. However, this is not the case. We have recorded the magnetization under the same experimental conditions as for the

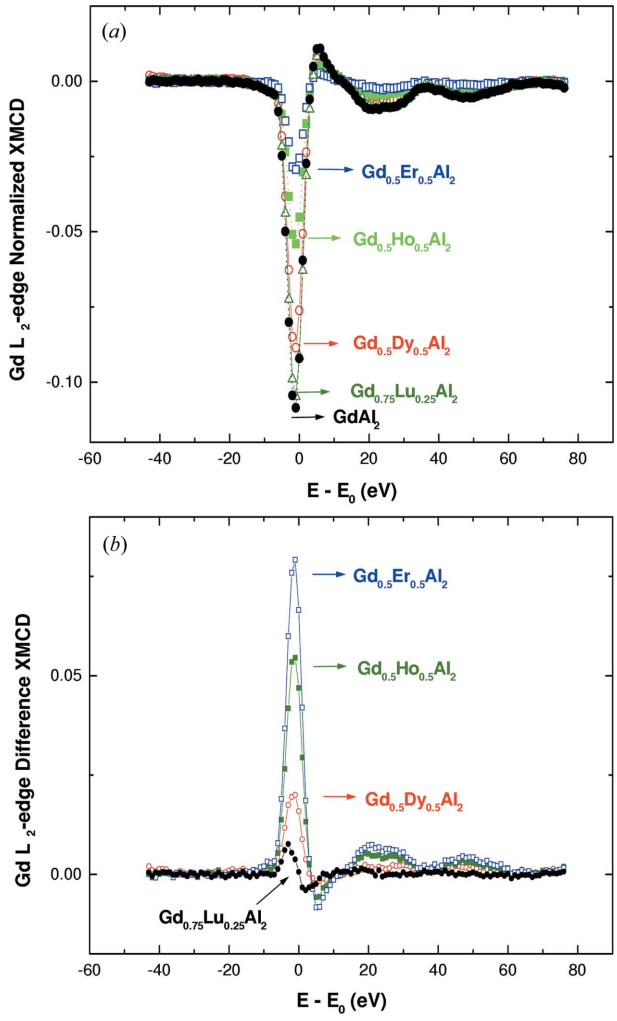

Figure 4
(*a*) Comparison of the XMCD spectra recorded at $T = 50$ K at the Gd L_2-edge in the case of $GdAl_2$ (black, filled circles), the $Gd_{0.5}R'_{0.5}Al_2$ compounds with R' = Er (blue, open squares), Ho (green, filled squares), Dy (red, open circles), and in $Gd_{0.75}Lu_{0.25}Al_2$ (dark green, open triangles). (*b*) Comparison of the XMCD spectra recorded at $T = 50$ K at the Gd L_2-edge in the $Gd_{0.5}R'_{0.5}Al_2$ compounds after subtracting the XMCD of the $GdAl_2$ one: R' = Er (blue, open squares), Ho (green, filled squares), Dy (red, open circles), and in $Gd_{0.75}Lu_{0.25}Al_2$ (black, filled circles). This figure is in colour in the electronic version of this paper.

XMCD measurements, *i.e.* $T = 50$ K and $H = 2$ T, verifying that a similar relation holds. Under these conditions the magnetization of $GdAl_2$, $Gd_{0.5}Dy_{0.5}Al_2$, $Gd_{0.5}Ho_{0.5}Al_2$ and $Gd_{0.75}Lu_{0.25}Al_2$ is ~86% of that at $T = 4.2$ K and $H = 5$ T, while it is only ~60% in the case of $Gd_{0.5}Er_{0.5}Al_2$. Finally, it should also be noted that the variation of the XMCD intensity through the $Gd_{0.5}R'_{0.5}Al_2$ series does not follow that of the magnetic ordering temperature. Indeed, as shown in Table 1, the maximum variation should be expected for the $Gd_{0.5}Er_{0.5}Al_2$ compound for which $T_C/T_C(GdAl_2) \simeq 0.6$. By contrast, the ratio of the XMCD amplitude for this compound, $XMCD/XMCD(GdAl_2) = 0.25$, is significantly smaller than the ratio of the magnetic ordering temperatures.

Atempting to gain a deeper insight into this peculiar behaviour, we have considered our previous findings in the

case of RT_2 compounds in which T is a 3d transition metal such as Fe or Co. In these cases we have demonstrated that the transition metal contributes to the XMCD signals recorded at the rare-earth $L_{2,3}$-edges (Laguna-Marco *et al.*, 2005*b*, 2007*a*, 2008*a*,*b*), and, moreover, that this contribution is related to the molecular field owing to the transition metal acting at the rare-earth sites (Chaboy *et al.*, 2007*b*). Then, we have checked the possibility that the rare-earth substituting Gd in the $Gd_{0.5}R'_{0.5}Al_2$ compounds could also contribute to the XMCD of the Gd L-edges. The existence of such a contribution can be highlighted by subtracting the XMCD spectra of $GdAl_2$ from those of the $Gd_{0.5}R'_{0.5}Al_2$ compounds. The result of the substraction is reported in Fig. 4 for the case of the L_2-edge (similar results are found at the L_3-edge). In all cases, with the exception of Lu, the extracted signal shows a sharp positive peak at the edge. While its shape is the same for all of the compounds, the intensity shows marked differences as a function of the rare-earth (Dy, Ho, Er) that substitutes for Gd. While in the case of Lu this difference can be associated with a simple dilution effect, the magnitude of the differences found for the cases in which R is a magnetic rare-earth does not show a direct relationship with the magnetic moments. The maximum difference signal is found for the case of Er, its intensity being $\sim$1.5 and 4 times greater than those of Ho and Dy, respectively. As commented above, these differences cannot be easily accounted for in terms of the different magnetic moments of the rare-earths substituting Gd, *i.e.* $\mu_{R'} = 10\ \mu_B$ for Dy and Ho, and 9 μ_B for Er.

We have studied whether this contribution can be regarded as being due to the hybridization of the 5d states of both Gd and R' ions. In this way, the Gd 5d states will be polarized by the interatomic 4f–5d exchange but, in addition, the R' ions should also contribute to the polarization of the 5d band through the action of the interatomic molecular field. It should be noted that the sign of the XMCD spectra indicates the orientation of the magnetic moment of the states probed in the photoabsorption process with respect to the magnetization of the system. However, the XMCD signals recorded at the $L_{2,3}$-edges of the rare-earths yield an erroneous sign (Schütz *et al.*, 1988). Indeed, if one considers that the XMCD spectrum reflects the difference in the density of empty states with different spin moment, this model yields that the 5d spin would be antiparallel to the 4f spin, which is in contradiction with the current knowledge (Campbell, 1972; Yamada *et al.*, 1984; Yamada & Shimizu, 1985). This paradox has been solved by taking into account the spin dependence of the matrix elements previously neglected (Wang *et al.*, 1993). It should be noted that the $L_{2,3}$ XMCD returns the correct sign when the rare-earth does not exhibit a 4f magnetic moment and the 5d spin is induced by a transition metal or by another rare-earth showing a localized 4f moment. This is the case for the Lu $L_{2,3}$ XMCD in $LuFe_2$ and $Gd_{0.75}Lu_{0.25}Al_2$ compounds (Chaboy *et al.*, 2007*c*). In a similar way, the results reported in Fig. 4 indicate that the polarization of the 5d states associated with the R' atoms agrees with the ferromagnetic coupling of the Gd and R' magnetic moments in the $Gd_{0.5}R'_{0.5}Al_2$ compounds. In order to explore the relationship between the R' contribution to the Gd $L_{2,3}$ XMCD signals and the molecular field owing to the R' ions acting on the Gd sites, we have calculated $B_{mol}(R' \rightarrow Gd)$ within a mean-field approach (Buschow, 1988). In this model, the intersublattice molecular field coefficient describing the interaction between the two rare-earth sublattices is given by

$$N_{RR'} = \left(\frac{|T_C - T_R|\,|T_C - T_{R'}|}{C_R\, C_{R'}} \right)^{1/2}, \qquad (1)$$

where $C_R = N_R g_J^2 J(J+1)\mu_B{}^2/3k_BT$, and T_R and $T_{R'}$ are the Curie temperatures of the RAl_2 and $R'Al_2$ compounds, respectively. The corresponding values of $N_{RR'}$ and B_{mol}, obtained as $B_{mol}(R' \rightarrow Gd) = N_{GdR'}\mu_{R'}$, are listed in Table 2.

Table 2
Intersublattice molecular coefficient and molecular field that the R' atoms exerts on the Gd sites.

Compound	$N_{RR'}$ (10^{-5} T m A^{-1})	B_{mol} ($R' \rightarrow$ Gd) (T)
$Gd_{0.5}Dy_{0.5}Al_2$	3.7	7.1
$Gd_{0.5}Ho_{0.5}Al_2$	4.7	8.9
$Gd_{0.5}Er_{0.5}Al_2$	5.8	10.0

As we can see in Table 2, the molecular field coefficient $N_{RR'}$ increases from Dy to Er as the maximum intensity of the subtracted Gd L_2 XMCD signal does. The $N_{RR'}$ increase reflects the variation of T_C observed along the $Gd_{1-x}R'_xAl_2$ series. In the case of Er, T_C increases from 13 K in $ErAl_2$ to 94 K in $Gd_{0.5}Er_{0.5}Al_2$, that is $\Delta T_C = 81$ K, which corresponds to a $\sim$623% increase. In the Ho series, T_C increases from 29 K in $HoAl_2$ to 101 K in $Gd_{0.5}Ho_{0.5}Al_2$, or equivalently, $\Delta T_C = 72$ K, which corresponds to an increase of $\sim$248%, whereas in the case of Dy this increase is only $\sim$98% as T_C increases from 58 K in $DyAl_2$ to 115 K in $Gd_{0.5}Dy_{0.5}Al_2$. That is, the values of T_C indicate that the exchange interaction between Gd and R' increases from Dy to Er. Finally, the obtained values of $B_{mol}(R' \rightarrow Gd)$ have been compared in Fig. 5 with the intensity of the subtracted Gd L_2 XMCD signals. The good agreement shown in this figure gives support to our hypothesis regarding the relationship between the XMCD and the molecular field acting on the absorbing sites.

The magnitude of the subtracted Gd L_2 XMCD signals deserves a final comment, being of the same order of magnitude as those previously found in the RFe_2 systems (Laguna-Marco *et al.*, 2008*a*). In this respect, it should be noted that when applying the procedure above we have subtracted the same Gd L_2 XMCD signal of $GdAl_2$ recorded at $T = 50$ K as those of the $Gd_{0.5}R'_{0.5}Al_2$ compounds recorded under the same conditions. However, this temperature ($T = 50$ K) is not so far from the magnetic ordering temperatures of the substituted $Gd_{0.5}R'_{0.5}Al_2$ compounds and, consequently, this approach might no longer be valid. Indeed, the magnetization measured at $T = 50$ K and $H = 5$ T is 6.09 μ_B/f.u. and 7.95 μ_B/f.u. for $GdAl_2$ and $Gd_{0.5}Dy_{0.5}Al_2$, respectively, yielding a $M_{5T}(50\text{ K})/M_{5T}(4.2\text{ K})$ ratio of 0.9. This ratio decreases to 0.8 for $Gd_{0.5}Ho_{0.5}Al_2$ [$M_{5T}(50\text{ K}) = 6.83\ \mu_B$/f.u.] and to 0.7 in the case of $Gd_{0.5}Er_{0.5}Al_2$ [$M_{5T}(50\text{ K}) = 5.32\ \mu_B$/f.u.]. These results

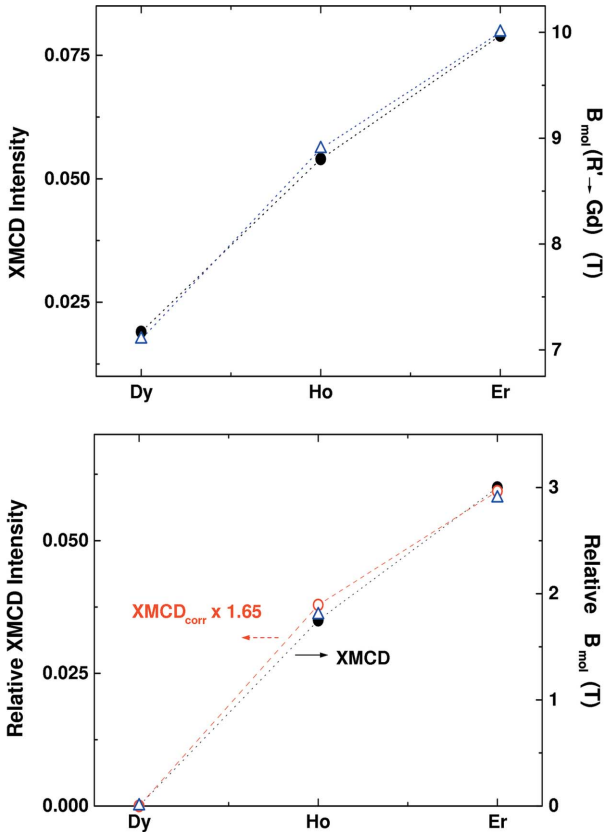

Figure 5
Top: comparison of the maximum intensity of the difference XMCD spectra (black, filled circles) and the intersublattice molecular field (blue, open triangles) through the $Gd_{0.5}R'_{0.5}Al_2$ series (see text for details). Bottom: comparison of the relative maximum intensity of the difference XMCD spectra prior (black, filled circles) and after applying the magnetization correction (red, open circles) (see text for details) and the relative variation of the intersublattice molecular field (blue, open triangles) through the $Gd_{0.5}R'_{0.5}Al_2$ series. This figure is in colour in the electronic version of this paper.

suggest that subtracting the XMCD signal of $GdAl_2$ from the XMCD signals of the $Gd_{0.5}R'_{0.5}Al_2$ compounds is appropriate for the Dy case, but probably not for the Ho and Er cases. Consequently, we have modified the subtraction procedure by taking into account these factors. In this way, the $GdAl_2$ signal has been factorized by 0.8/0.9 and 0.7/0.9 prior to subtracting it from the XMCD spectra of the Ho and Er compounds, respectively. The result of such a procedure is incorporated in the bottom panel of Fig. 5. As shown in the figure, while the magnitude of the extracted signal is reduced, the trend of the intensity variation through the substituted series does not vary. As a consequence, a comparison of the intensity of the extracted XMCD signals and the value of the intersublattice molecular field also shows a remarkable agreement.

After applying this correction we found that the intensity of the extracted XMCD signals in the $Gd_{0.5}R'_{0.5}Al_2$ compounds is about a half of that found in the RFe_2 series, while the intersublattice molecular field is about five times smaller (applying the same procedure as discussed above yields $B_{mol} = 45.4$ T for $GdFe_2$). These differences are presumably due to the different hybridization mechanism occurring in both $R_{0.5}R'_{0.5}Al_2$, $R(5d)$–$R'(5d)$, and RFe_2, $R(5d)$–Fe($3d$), systems. The present results suggest that, while the magnitude of the discussed effect on the XMCD spectra is determined by the details of the interplay of the hybridization and the spin polarization of the $R(5d)$ states, the relative variation through the same series is mainly determined by the molecular field acting on the rare-earth absorbing sites.

4. Summary and conclusions

We have presented here an XMCD study performed at the rare-earth $L_{2,3}$-edges in the case of $R_xR'_{1-x}Al_2$ compounds. It is shown that both R and R' atoms contribute to the XMCD recorded at the L-edges of the selected rare-earth. In the case of the $Gd_xR'_{1-x}Al_2$ compounds, we have extracted the contribution of R' to the Gd $L_{2,3}$-edges XMCD spectra. We have shown that the variation of the intensity of this contribution through the series is determined by the molecular field owing to the R' atoms acting on the Gd sites. These results close a longstanding study on the origin and the interpretation of the $L_{2,3}$-edge XMCD spectra of the rare-earths in the case of multi-component magnetic systems.

This work was partially supported by a Spanish CICYT-MAT2008-06542-C04-01 grant. MALM and RB acknowledge the Ministerio de Eduación y Ciencia of Spain for a Post-doctoral and a PhD grant, respectively. This study was performed with the approval of Japan Synchrotron Radiation Research Institute (JASRI) (Proposals No. 1999A0388 and 2001A0062).

References

Boada, R., Laguna-Marco, M. Á. & Chaboy, J. (2009). *J. Synchrotron Rad.* **16**, 38–42.
Boada, R., Piquer, C., Laguna-Marco, M. A., Kawamura, N., Suzuki, M. & Chaboy, J. (2009). *Phys. Rev. B.* Submitted.
Burd, J. & Lee, E. W. (1977). *J. Phys. C*, **10**, 4581–4586.
Buschow, K. H. J. (1979). *Rep. Prog. Phys.* **42**, 1374–1477.
Buschow, K. H. J. (1988). In *Handbook of Magnetic Materials*, Vol. 4, edited by K. H. J. Buschow, ch. 1. Amsterdam: Elsevier Science.
Campbell, I. A. (1972). *J. Phys. F*, **2**, L47–L50.
Carra, P., Harmon, B. N., Thole, B. T., Altarelli, M. & Sawatzky, G. A. (1991). *Phys. Rev. Lett.* **66**, 2495–2498.
Carra, P., Thole, B. T., Altarelli, M. & Wang, X. (1993). *Phys. Rev. Lett.* **70**, 694–697.
Chaboy, J., Bartolomé, F., García, L. M. & Cibin, G. (1998*a*). *Phys. Rev. B*, **57**, R5598–R5601.
Chaboy, J., García, L. M., Bartolomé, F., Maruyama, H., Marcelli, A. & Bozukov, L. (1998*b*). *Phys. Rev. B*, **57**, 13386–13389.
Chaboy, J., Laguna-Marco, M. A., Maruyama, H., Ishimatsu, N., Isohama, Y. & Kawamura, N. (2007*a*). *Phys. Rev. B*, **75**, 144405.
Chaboy, J., Laguna-Marco, M. Á., Piquer, C., Boada, R., Maruyama, H. & Kawamura, N. (2008). *J. Synchrotron Rad.* **15**, 440–448.
Chaboy, J., Laguna-Marco, M. A., Piquer, C., Maruyama, H. & Kawamura, N. (2007*b*). *J. Phys. Condens. Matter*, **19**, 436225.
Chaboy, J., Laguna-Marco, M. A., Piquer, C., Maruyama, H., Kawamura, N., Ishimatsu, N., Suzuki, M. & Takagaki, M. (2007*c*). *Phys. Rev. B*, **75**, 064410.

Chaboy, J., Laguna-Marco, M. A., Sánchez, M. C., Maruyama, H., Kawamura, N. & Suzuki, M. (2004). *Phys. Rev. B*, **69**, 134421.
Chaboy, J., Maruyama, H., García, L. M., Bartolomé, J., Kobayashi, K., Kawamura, N., Marcelli, A. & Bozukov, L. (1996). *Phys. Rev. B*, **54**, R15637–R15640.
Chaboy, J., Piquer, C., Plugaru, N., Artigas, M., Maruyama, H., Kawamura, N. & Suzuki, M. (2003). *J. Appl. Phys.* **93**, 475–478.
Chaboy, J., Piquer, C., Plugaru, N., Bartolomé, F., Laguna-Marco, M. A. & Plazaola, F. (2007*d*). *Phys. Rev. B*, **76**, 134408.
Chen, C. T., Idzerda, Y. U., Lin, H.-J., Meigs, G., Chaiken, A., Prinz, G. A. & Ho, G. H. (1993). *Phys. Rev. B*, **48**, 642–645.
Crocombettey, J. P., Thole, B. T. & Jollet, F. (1996). *J. Phys. Condens. Matter*, **8**, 4095–4105.
Funk, T., Deb, A., George, S. J., Wang, H. & Cramer, S. P. (2005). *Coord. Chem. Rev.* **249**, 3–30.
Gennes, P. G. de (1966). *C. R. Acad. Sci. (Paris)*, **247**, 1836–1838.
Giorgetti, C., Dartyge, E., Baudelet, F. & Galéra, R.-M. (2004). *Phys. Rev. B*, **70**, 035105.
Goering, E. (2005). *Philos. Mag. B*, **85**, 2895–2911.
Igarashi, J. & Hirai, K. (1994). *Phys. Rev. B*, **50**, 17820–17829.
Igarashi, J. & Hirai, K. (1996). *Phys. Rev. B*, **53**, 6442–6450.
Ishimatsu, N., Miyamoto, S., Maruyama, H., Chaboy, J., Laguna-Marco, M. A. & Kawamura, N. (2007). *Phys. Rev. B*, **75**, 180402.
Kortright, J. B., Awschalom, D. D., Stöhr, J., Bader, S. D., Idzerda, Y. U., Parkin, S. S. P., Schuller, I. K. & Siegmann, H.-C. (1999). *J. Magn. Magn. Mater.* **207**, 7–44.
Laguna-Marco, M. A. (2007). Editor. *A New Insight into the Interpretation of the T K-edge and R $L_{2,3}$-Edges XMCD Spectra in R–T Intermetallics.* Zaragoza: Prensas Universitarias de Zaragoza.
Laguna-Marco, M. A., Chaboy, J. & Maruyama, H. (2005*a*). *Phys. Rev. B*, **72**, 094408.
Laguna-Marco, M. A., Chaboy, J. & Piquer, C. (2008*a*). *Phys. Rev. B*, **77**, 125132.
Laguna-Marco, M. A., Chaboy, J. & Piquer, C. (2008*b*). *J. Appl. Phys.* **103**, 07E141.
Laguna-Marco, M. A., Chaboy, J., Piquer, C., Maruyama, H., Ishimatsu, N. & Kawamura, N. (2007*a*). *AIP Conf. Proc.* **882**, 484–486.
Laguna-Marco, M. A., Chaboy, J., Piquer, C., Maruyama, H., Ishimatsu, N., Kawamura, N., Takagaki, M. & Suzuki, M. (2005*b*). *Phys. Rev. B*, **72**, 052412.
Laguna-Marco, M. A., Chaboy, J., Piquer, C., Maruyama, H., Kawamura, N. & Takagaki, M. (2007*b*). *J. Magn. Magn. Mater.* **316**, e425–e427.
Laguna-Marco, M. A., Piquer, C. & Chaboy, J. (2009). *Phys. Rev. B.* Submitted.
Lang, J. C., Kycia, S. W., Wang, X. D., Harmon, B. N., Goldman, A. I., Branagan, D. J., McCallum, R. W. & Finkelstein, K. D. (1992). *Phys. Rev. B*, **46**, 5298–5302.
Lang, J. C., Srajer, G., Detlefs, C., Goldman, A. I., König, H., Wang, X., Harmon, B. N. & McCallum, R. W. (1995). *Phys. Rev. Lett.* **74**, 4935–4938.
Lang, J. C., Wang, X., Harmon, B. N., Goldman, A. I., Dennis, K. W., McCallum, R. W. & Finkelstein, K. D. (1994). *Phys. Rev. B*, **50**, 13805–13808.
Lovesey, S. W. & Collins, S. P. (1996). Editors. *X-ray Scattering and Absorption by Magnetic Materials.* London: Clarendon.
Maruyama, H. (2001). *J. Synchrotron Rad.* **8**, 125–128.
Purwins, H. G. & Leson, A. (1990). *Adv. Phys.* **39**, 309–405.
Rodriguez-Carvajal, J. (1993). *Physica B*, **192**, 55–69.
Rueff, J. P., Galéra, R. M., Giorgetti, C., Dartyge, E., Brouder, C. & Alouani, M. (1998). *Phys. Rev. B*, **58**, 12271–12281.
Scherz, A., Wende, H. & Baberschke, K. (2004). *Appl. Phys. A*, **78**, 843–846.
Schütz, G., Frahm, R., Wienke, R., Wilhelm, W., Wagner, W. & Kienle, P. (1989). *Rev. Sci. Instrum.* **60**, 1661–1665.
Schütz, G., Wagner, W., Wilhelm, W., Kienle, P., Zeller, R., Frahm, R. & Materlik, G. (1987). *Phys. Rev. Lett.* **58**, 737–740.
Schütz, G. & Wienke, H. (1989). *Hyperfine Interact.* **50**, 457–476.
Schütz, G., Wienke, R., Knülle, M., Wilhelm, W., Wagner, W., Kienle, P. & Frahm, R. (1988). *Z. Phys. B*, **73**, 67–75.
Stähler, S., Schütz, G. & Ebert, H. (1993). *Phys. Rev. B*, **47**, 818–826.
Stöhr, J. (1999). *J. Magn. Magn. Mater.* **200**, 470–497.
Suzuki, M., Kawamura, N., Mizumaki, M., Urata, A., Maruyama, H., Goto, S. & Ishikawa, T. (1998). *Jpn. J. Appl. Phys.* **37**, L1488–L1490.
Thole, B. T., Carra, P., Sette, F. & van der Laan, G. (1992). *Phys. Rev. Lett.* **68**, 1943–1946.
Wang, X., Leung, T. C., Harmon, B. N. & Carra, P. (1993). *Phys. Rev. B*, **47**, 9087–9090.
Yamada, H., Inoue, J., Terao, K., Kanda, S. & Shimizu, M. (1984). *J. Phys. F*, **14**, 1943–1960.
Yamada, H. & Shimizu, M. (1985). *J. Phys. F*, **15**, L175–L180.